Reply to Reviewer #2 comments

The authors would like to thank anonymous reviewer #2 for taking the time to review this manuscript and providing valuable comments and recommendations on an open discussion. For the ease of cross reading, authors responses are given under the reproduced version of each comment by reviewer #2. Each of the comments from the reviewer are numbered and the changes made in the manuscript are shown using a red font under the authors response given in blue font.

Comments

1. *The authors review the airborne polarimeters (SPEX, RSP, AirMSPI). It is also necessary to review aerosol retrieval algorithms used by these sensors and published elsewhere.*

References to the current retrieval algorithms used by different sensors have been added to the revised manuscript. Also redirecting the readers to more comprehensive review papers on polarimetric aerosol sensing and retrieval algorithms.

Changes implemented in Section 1,

~~For~~There are several aerosol retrieval algorithms specifically optimized for MAPs which includes: SRON multi-mode inversion algorithm for SPEX airborne (Fu et al., 2020; Fu and Hasekamp, 2018); Microphysical Aerosol Property from Polarimeters (MAPP) (Stamnes et al., 2018) and GISS/RSP algorithm (Knobelspiesse et al., 2011; Waquet et al., 2009) for RSP; correlated multi-pixel and joint retrieval algorithm for AirMSPI developed at Jet Propulsion Laboratory (JPL) (Xu et al., 2017, 2019). This list is not complete, for a comprehensive review of the polarimetric remote sensing of atmospheric aerosols based on MAPs, we encourage the readers to refer to several reviews in the literature (Dubovik et al., 2019; Kokhanovsky et al., 2015; Remer et al., 2019).

2. *Associated with the comparison of AirHARP AOD results against AERONET reference data in Figure 14, how do the comparison of single scattering albedo and non-spherical particle fraction look like? Though the AOD loading is low, are we still able to see a trend of improved agreement of these properties as AOD increases?*

Since the aerosol loading is very low, most of the AERONET stations do not have SSA retrievals for many of the collocated observations. For those AERONET stations that do have a retrieval for SSA are only at Level1.5, which are not quality assured. There are 6 collocated observations for the SSA. A comparison plot for the GRASP retrieved SSA using AirHARP observation and L1.5 SSA retrieved using AERONET almucantar measurements is given in Fig. AR2.1. The figure also includes the plot which shows the trend of difference in SSA with an increase in the AOD measured by the AERONET. The same plots are given for two cases: a) five modal log-normal size distribution based GRASP/Five mode kernel and b) aerosol component-based GRASP/Models kernel where complex refractive index, spherical fraction and aerosol distribution are fixed. Only the weight for each aerosol components can change in the retrieval. There is a significant reduction in the number of retrieved aerosol parameters from 15 to 6 in case (b), which will reduce the non-linearity of the minimization problem. In the Reply to Reviewer #1, we show an analysis that demonstrates that the

sensitivity to the spherical fraction is small for fine mode dominated particle size distribution and we can't expect a good agreement with the AERONET retrieved SF.

The point is that there is insufficient aerosol loading with the AERONET match-ups to expect a good retrievals of particle properties from any inversion. This is why AERONET has no Level 2 Quality Assured retrievals, and why we do not want to include any comparisons in the paper.
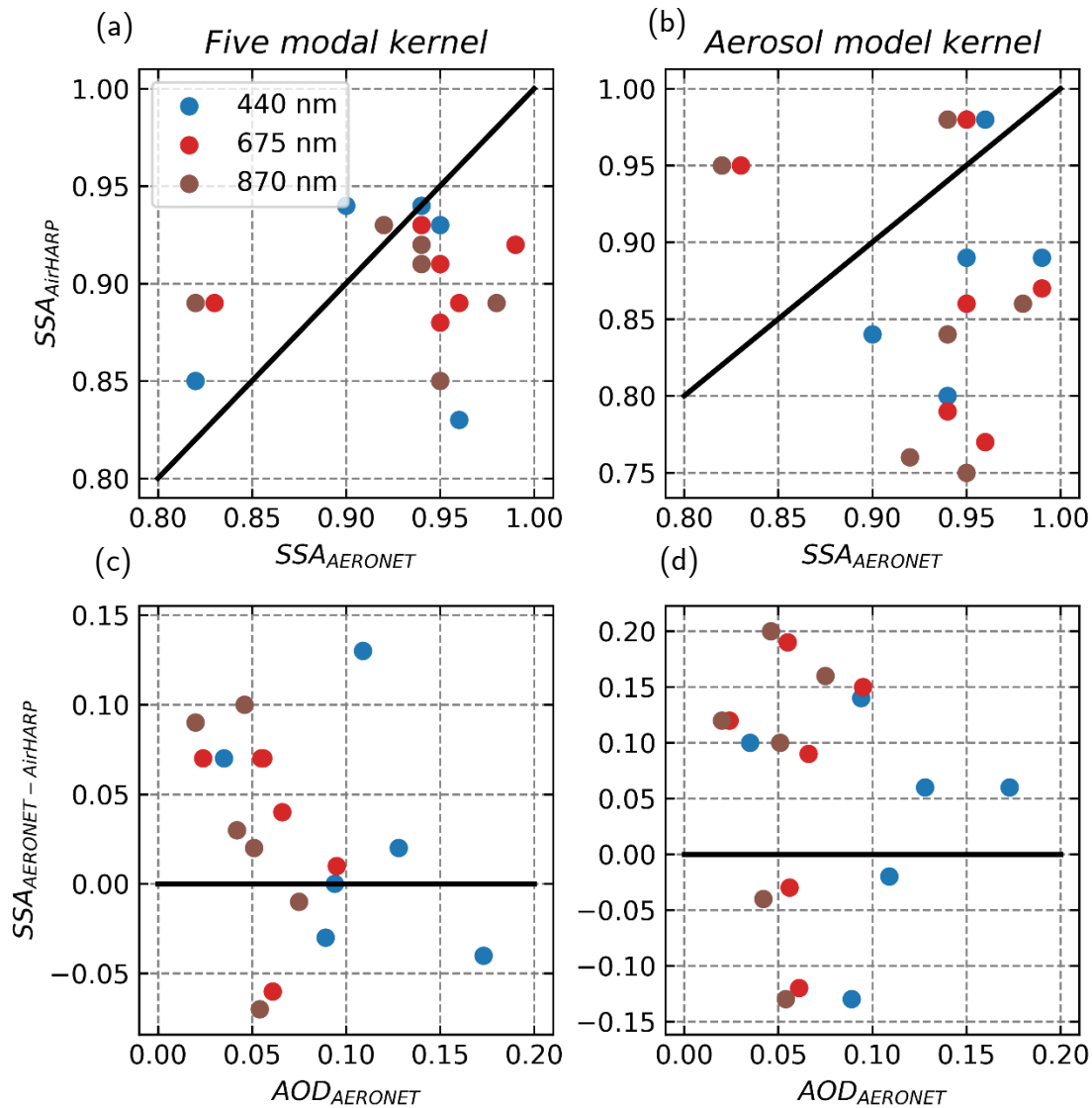
Figure AR2.1: (a) and (b) are the scatter plots of retrieved SSA from AERONET and AirHARP observations. For the case of (a), AirHARP retrievals use a GRASP five modal log-normal kernel, where the complex refractive index and spherical fraction are retrieved along with the weight for each lognormal mode in the PSD (See Table. 3 in the manuscript for more details on the fixed size modes). On the other hand, case (b) uses an aerosol type-based GRASP kernel where optical properties are precomputed using different aerosol types mentioned in Table. 6. Subplots (c) and (d) show the trend of difference in SSA retrieved from AERONET and AirHARP observations with an increase in AOD measured by AERONET stations. Plots (c) and (d) are based on the kernels mentioned in (a) and (b) respectively.

3. The authors need to be clearer on the adoption of size components in AirHARP retrieval. Table 3 and Table 6 give two different size components in retrieval. If I

understand well, size components in Table 3 are the default option in GRASP while size components in Table 6 were created for AirHARP retrieval. What is the difference in retrieval based on these two different assumptions? Which one gives a better fit to AERONET AOD and SSA? As the authors pointed out "This simplified approach significantly drops the complexity of the aerosol model by reducing the number of parameters retrieved in the joint retrieval. It helps in reducing the nonlinearity of the inverse problem and makes the separation of the surface and aerosol signal much less complicated compared to a five-lognormal mode kernel." However, would it also possible that the size components in Table 6 (with a fixed refractive index for each mode) also increase the risk of getting more subjection to pre-determined aerosol modeling errors? If so, how large is the modeling error?

Table 3 is the default option used for the retrieval in this paper. It is not the default option in GRASP. GRASP offers many options. Its most generalized version of a kernel has 22 bins for the particle size distribution plus all of the other particle properties. But to reduce the complexity for the AirHARP retrievals, based on the experience of PARASOL/GRASP retrievals, we are using a different option with the predefined five modal log-normal distribution mentioned in Table 3. This one has 15 free parameters including spectrally dependent complex refractive index, spherical fraction, etc. For the AERONET comparison, we invoke yet a different GRASP option. We used the GRASP/Models approach representing aerosol as an external mixture of predetermined aerosol components, where the number of free parameters is further reduced to 6 and the complex refractive index and the spherical fraction are fixed for each aerosol type. Only the concentration (weight) of each aerosol component in Table 4 (old Table 6) are retrieved during the inversion. Since the aerosol loading for the AERONET comparison cases is below 0.17, this approach seems to be working well compared to the one mentioned in Table 3 (complex refractive index and spherical fraction are retrieved parameters).

We have worked hard to try and clarify the text in this matter, and have added a plot (Figure 14 in the revised manuscript) that compares the 15 and 6 free parameter options.

Figure AR2.1 gives us an insight into modeling error because of the assumption of the aerosol components. For this range of aerosol loading, the assumption of aerosol type will not significantly affect the R_I, and *DoLP* calculations. However, this assumption may not hold for higher aerosol loading where a predetermined aerosol model will create modeling error in R_I and *DoLP* calculated using the forward model.

Changes implemented in the manuscript relevant to this comment:

In section 3.2 describing the different GRASP kernels and surface models used in the retrievals,

The ~~particle~~ single-scattering ~~kernel~~calculations that we employ for the AirHARP retrieval ~~us-esuse~~ one of two possible retrieval set-ups: 1) five ~~fixed~~ log-normal distribution modes as described in Table 3~~.~~, or 2) the aerosol is assumed as an external mixture of five aerosol components as described in Table 4. Both approaches were extensively used in PARASOL/GRASP processing and, therefore, considered here. For the first kernel possibility, the retrieval has 15 aerosol parameters to retrieve and is called as "GRASP/Five mode" kernel. Each of ~~those~~the log-normal modes has a fixed mode radius and width. The ~~only~~ free parameter in the retrieval for particle size distribution is the concentration of particles in each bin. There are three lognormal modes in the fine mode ~~and two in the coarse mode.~~(log-normal modes 1 to 3 in

Table 3) and two in the coarse mode (log-normal modes 4 and 5 in Table 3). Other retrieved parameters related to aerosol properties include a complex refractive index, aerosol layer height, and the fraction of spherical particles (SF). The same kernel is used for all the retrievals in this paper with an exception for the AERONET comparison mentioned in Section 5.2. For the AERONET comparison, we make use of the second GRASP kernel that has reduced the number of aerosol parameters from 15 to 6. This reduced parameter option is the "GRASP/Models" kernel, where particle properties are assumed for each aerosol components given in Table 4. Complex refractive index, SF, and particle size distribution of each aerosol components are fixed for this kernel. Only the concentration (weight) for each aerosol component is retrieved.

Another change in the same section,

The state vector *a* includes the information on particle size distribution which is the concentration for five log-normal modes of Table 3, the complex refractive index in the four spectral bands that are independent of particle size, the fraction of spherical particles (SF), aerosol layer height, and parameters characterizing the directional reflectance of the surface. AOD is derived from retrieved aerosol properties using the method mentioned in appendix B.1. Additionally, fine mode AOD is calculated using modes 1-3 mentioned in Table 3 and coarse mode AOD using modes 4 and 5. Single Scattering Albedo (SSA), Angstrom Exponent (AE) are also derived from the retrieved aerosol properties. For the GRASP/Models approach, the state vector *a* includes the concentration for each aerosol component mentioned in Table 4. State vector *a* does not contain information on the particle size distribution, SF, and complex refractive index. All this is embedded in the aerosol components which ~~which includes the aerosol types:~~ are close (with some modifications) to biomass burning, urban, urban polluted, maritime, and desert dust observed in AERONET climatology by ~~(~~Dubovik et al., 2002~~)~~. Among these, only desert dust is considered as completely non-spherical, and similarly to AERONET retrievals, uses a shape distribution mentioned in ~~(~~Dubovik et al., 2006~~)~~. All the other types are treated as 100 % spherical particles. The details of the bi-modal size distribution parameters along with the fixed complex refractive index for each of the aerosol component~~types~~ are tabulated in Table 4~~6~~ and are based on the work of Dubovik et al., 2002. Figure 1~~3~~ shows the particle size distribution as a function of radii for the different aerosol component~~types~~. The main differences between ~~the five log normal mode kernel~~ GRASP/Five mode and GRASP/Models approach~~based retrievals~~ are, 1.) instead of retrieving the concentration of each log-normal mode, concentration(weight) for each of the aerosol components mentioned in ~~the~~ Table 4~~6~~ are retrieved. 2) RRI, IRI, and SF are not retrieved since these are fixed for each of the aerosol components. This simplified approach significantly drops the complexity of the aerosol model by reducing the number of parameters retrieved directly in the joint retrieval. It helps in reducing the nonlinearity of the inverse problem and makes the separation of the surface and aerosol signal much less complicated compared to the GRASP/Five mode approach~~a five lognormal mode kernel~~. At the same time, all aerosol total properties as SSA, effective size distribution, complex refractive index can be obtained using external aerosol mixture concept. The reduction of sought unknowns helps situations in lower information content (e.g., for low AOD) and makes the separation of the surface and aerosol signal much less complicated compared to a GRASP/Five mode kernel. This tendency is well identified in the in-depth analysis of PARASOL data processing using different retrieval setups by Chen et al. 2020 (In preparation). Like the GRASP/Five mode kernel, the state vector *a* includes the information on aerosol layer height. Even though aerosol layer height is retrieved during the retrieval process, the sensitivity

to aerosol height for the AirHARP wavelengths is negligible for most of the low loading cases. Retrieved aerosol layer height is thus not discussed in this work.

Retrieval of aerosol properties from MAPs is highly sensitive to the accurate representation of the directional reflectance from the surface. For the ocean pixels, the ~~The ocean~~ surface model used is the NASA GISS model (Mishchenko and Travis, 1997) based on Cox and Munk (1954), in which the ocean surface reflectance is represented by three parameters: ocean surface albedo, the fraction of Fresnel reflection surface, and wind speed denoted by a_0, a_1, and a_2 respectively, with details given in Appendix A.2. These three parameters are the surface components in the state vector a for the case of ocean pixels. For the case of land pixel, Ross-Thick Li-Sparse linear BRDF model is used to represent the directional reflectance from the surface (see Appendix A.1.1), which uses three parameters K_0, K_1, K_2. K_0 is a spectrally dependent parameter that represents the isotropic reflectance, K_1 and K_2 normalized to K_0 are the spectrally independent parameters which are the coefficient of geometric and volumetric scattering kernels respectively (Maignan et al., 2004; Wanner et al., 1995). Polarized reflectance from the surface is modeled using the Maignan-Breon one-parameter ~~α~~model and the retrieved parameter is a scaling factor (α) that is spectrally dependent (Maignan et al., 2009). Refer to Appendix A.1.2 for detailed information on the surface models. The four parameters K_0, K_1/K_0, K_2/K_0, and α are the surface components in the state vector a for the case of land pixels. In the next section, we discuss the results of applying GRASP to AirHARP measurements of R, Q/I and U/I for selected cases from the ACEPOL campaign.

In section 5.2 discussing the two aerosol GRASP kernel approaches and the results,

AirHARP observations in this validation exercise are retrieved with two versions of the GRASP aerosol kernels, one using the GRASP/Five mode kernel with 15 free parameters (Table 3) that allows for retrieval of particle properties, and the other using the GRASP/Models kernel with only 6 free parameters (Table 4) that restricts the particle properties to focus on the AOD retrieval. When aerosol loading is low, there is insufficient signal to retrieve particle properties. Allowing for additional free parameters without having sufficient signal will degrade the accuracy of the AOD retrieval. The maximum AOD measured by a collocated AERONET station during the ACEPOL campaign is 0.158 at 440 nm suggesting that in this exercise the simplified aerosol component model would be preferred over using the option with a greater number of free parameters. This is evident in the two figures, Fig. 14(a) and Fig. 14(b). Figure 14 shows the scatterplot ~~of these two data sets~~ with AOD$_{\mathrm{AERONET}}$ in the X-axis and AOD$_{\mathrm{AirHARP}}$ on the Y-axis. The spatial standard deviation of AOD within this 5.5 km x 5.5 km box is indicated using the error ~~bar~~bars in Fig. 14. Statistical parameters that represent the correlation between these two data sets are tabulated in the table inside ~~Fig. 14. The black dashed lines in Fig. 14 are AOD(1:1) ± 0.04 lines. Mean absolute error of 0.014, 0.013, 0.013 and 0.017~~the plots. In Fig. 14 a, for the case of AOD retrievals based on the GRASP/Five mode kernel with the greater number of free parameters, MAE of 0.041, 0.039, 0.037, 0.035 are obtained for the ~~spectral bands~~ 440, 550, 670, and 870 nm bands, respectively~~, with~~. The bias ranges from 0.022 to 0.038, with the 440 nm band having the largest bias and the 870 nm band ~~having~~ with the least. However, in Fig. 14b, for the case using the GRASP/Models kernel with the reduced number of free parameters, mean absolute error of 0.010, 0.010, 0.011, and 0.015 are obtained for the spectral bands 440, 550, 670, and 870 nm, respectively, with 870 nm band having a slightly higher spread than the other bands. Also, a similar trend is seen for 870 nm in the case of BIAS, where the 440, 550, and 670 nm ~~band~~bands have a BIAS of -0.~~011, 0.013,~~002, -0.~~011~~003, -0.004, respectively whereas 870 nm has a BIAS of -0.~~017. At low AOD we~~

~~can see a low bias compared to AERONET AOD measurements, which is similar to what we see for RSP vs AERONET comparison in (Fu et al., 2020).~~.009. Figure 14 demonstrates the need to match the appropriate kernel to the available information in the scene and to not attempt the retrieval of more free parameters than the aerosol loading permits. Overall, the performance of the AirHARP observations plus the GRASP retrieval algorithm gives a good ~~correlation~~agreement with the collocated AERONET observations~~.~~ especially when GRASP/Models kernel is used. The above tendency is well identified in the in-depth analysis of PARASOL data processing using different retrieval setups by Chen et al. 2020 (In preparation).

Updated Fig. 14 that plots the AirHARP AOD comparison with AERONET observations,

(a)   (b)
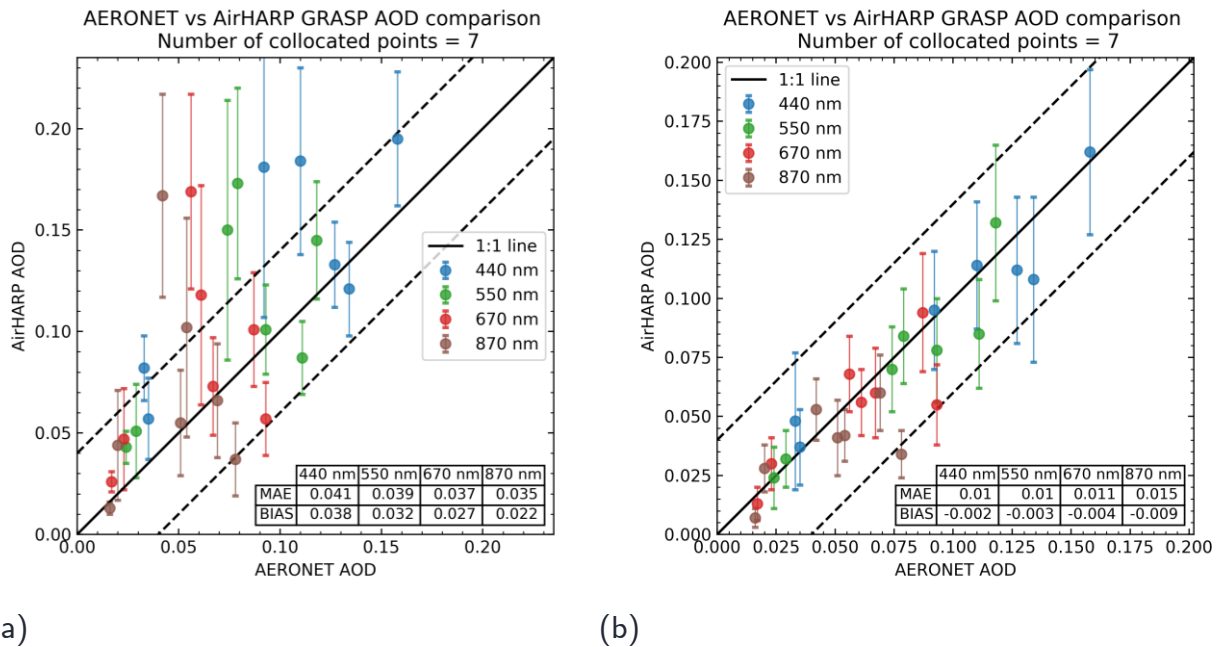
Figure 14. ~~Scattergram~~Scattergrams of aerosol optical depth (AOD) retrieved using Air-HARP observations over collocated AERONET ~~pixels~~stations vs AERONET measured AOD interpolated ~~at~~to AirHARP spectral bands. ~~A~~Plotted are the areal mean AirHARP AODs calculated from all the qualified retrievals within a box of 5.5km x 5.5km around the AERONET station against the collocated AERONET ~~pixel is used to calculate the spatial mean AOD (solid colored circles) over AERONET station using the AirHARP AOD retrievals.~~temporal mean AOD. Each colored error ~~bars indicate~~bar indicates the standard deviation of AOD within the ~~matching~~areal box. Mean Absolute Error (MAE) and BIAS for each spectral band are provided in the table inside the scattergram. ~~Black~~The black solid lines in the plots are the 1:1 lines and the dashed lines ~~in~~are ± 0.04 AOD from the ~~plot are~~1:1 line~~ ± 0.04~~. (a) GRASP retrievals using the fixed five modal log-normal GRASP kernel (Table 3) that has 15 free parameters and allows for retrieval of particle properties along with AOD (b) same as (a) except using the GRASP/Models approach (Table 4) that reduces free parameters to 6 and fixes particle properties based on the Table 4 and only retrieves the weight for each aerosol type.

In situations with low aerosol loading (AOD ¡ 0.17) over land, a simplified retrieval approach based on GRASP/Models kernel approximating aerosol as an external mixture of five aerosol components is also used for the AOD retrievals. One advantage of using this simplified kernel is that it retrieves a significantly smaller number of aerosol parameters compared to the standard GRASP/Five mode kernel and performed well for low aerosol loading cases in an AERONET comparison, despite the simplifying assumption of prescribed complex refractive index for each aerosol component. AOD retrieved from AirHARP using GRASP, matches collocated AERONET observations to within +0.~~005~~018/-0.~~025~~04 with a minimum MAE of 0.01 in 440 and 550 nm bands and maximum of 0.015 in the 870 nm spectral band. Thus, we note an overall low bias of -0.~~011~~002 to -0.~~017~~009, depending on wavelength..

> 4. As the AOD loading during the ACEPOL field campaign is low, it provides a very good testbed for surface retrieval. Is there any comparison of surface BRDF and pBRDF as retrieved from AirHARP and other sensors such as SPEX, RSP, and AirMSPI?

The authors agree with the reviewer that this dataset/campaign is a good testbed for surface retrieval. This is an ongoing project and will be part of a publication expected from that project. For now, the authors believe that it is beyond the scope of this paper.

References

Cox, C. and Munk, W.: Measurement of the Roughness of the Sea Surface from Photographs of the Sun's Glitter, J. Opt. Soc. Am., 44(11), 838, doi:10.1364/JOSA.44.000838, 1954.

Dubovik, O., Holben, B., Eck, T. F., Smirnov, A., Kaufman, Y. J., King, M. D., Tanré, D. and Slutsker, I.: Variability of Absorption and Optical Properties of Key Aerosol Types Observed in Worldwide Locations, J. Atmos. Sci., 59(3), 590–608, doi:10.1175/1520-0469(2002)059¡0590:VOAAOP¿2.0.CO;2, 2002.

Dubovik, O., Sinyuk, A., Lapyonok, T., Holben, B. N., Mishchenko, M., Yang, P., Eck, T. F., Volten, H., Muñoz, O., Veihelmann, B., van der Zande, W. J., Leon, J. F., Sorokin, M. and Slutsker, I.: Application of spheroid models to account for aerosol particle nonsphericity in remote sensing of desert dust, J. Geophys. Res. Atmos., 111(11), doi:10.1029/2005JD006619, 2006.

Dubovik, O., Li, Z., Mishchenko, M. I., Tanré, D., Karol, Y., Bojkov, B., Cairns, B., Diner, D. J., Espinosa, W. R., Goloub, P., Gu, X., Hasekamp, O., Hong, J., Hou, W., Knobelspiesse, K. D., Landgraf, J., Li, L., Litvinov, P., Liu, Y., Lopatin, A., Marbach, T., Maring, H., Martins, V., Meijer, Y., Milinevsky, G., Mukai, S., Parol, F., Qiao, Y., Remer, L., Rietjens, J., Sano, I., Stammes, P., Stamnes, S., Sun, X., Tabary, P., Travis, L. D., Waquet, F., Xu, F., Yan, C. and Yin, D.: Polarimetric remote sensing of atmospheric aerosols: Instruments, methodologies, results, and perspectives, J. Quant. Spectrosc. Radiat. Transf., 224, 474–511, doi:10.1016/j.jqsrt.2018.11.024, 2019.

Fu, G. and Hasekamp, O.: Retrieval of aerosol microphysical and optical properties over land using a multimode approach, Atmos. Meas. Tech., 11(12), 6627–6650, doi:10.5194/amt-11-6627-2018, 2018.

Fu, G., Hasekamp, O., Rietjens, J., Smit, M., Di Noia, A., Cairns, B., Wasilewski, A., Diner, D., Seidel, F., Xu, F., Knobelspiesse, K., Gao, M., da Silva, A., Burton, S., Hostetler, C., Hair, J. and Ferrare, R.: Aerosol retrievals from different polarimeters during the ACEPOL campaign using a common retrieval algorithm, Atmos. Meas. Tech., 13(2), 553–573, doi:10.5194/amt-13-553-2020, 2020.

Knobelspiesse, K., Cairns, B., Redemann, J., Bergstrom, R. W. and Stohl, A.: Simultaneous retrieval of aerosol and cloud properties during the MILAGRO field campaign, Atmos. Chem. Phys., 11(13), 6245–6263, doi:10.5194/acp-11-6245-2011, 2011.

Kokhanovsky, A. A., Davis, A. B., Cairns, B., Dubovik, O., Hasekamp, O. P., Sano, I., Mukai, S., Rozanov, V. V., Litvinov, P., Lapyonok, T., Kolomiets, I. S., Oberemok, Y. A., Savenkov, S., Martin, W., Wasilewski, A., Di Noia, A., Stap, F. A., Rietjens, J., Xu, F., Natraj, V., Duan, M., Cheng, T. and Munro, R.: Space-based remote sensing of atmospheric aerosols: The multi-angle spectro-polarimetric frontier, Earth-Science Rev., 145, 85–116, doi:10.1016/j.earscirev.2015.01.012, 2015.

Maignan, F., Bréon, F. M. and Lacaze, R.: Bidirectional reflectance of Earth targets: Evaluation of analytical models using a large set of spaceborne measurements with emphasis on the Hot Spot, Remote Sens. Environ., 90(2), 210–220, doi:10.1016/j.rse.2003.12.006, 2004.

Maignan, F., Bréon, F. M., Fédèle, E. and Bouvier, M.: Polarized reflectances of natural surfaces: Spaceborne measurements and analytical modeling, Remote Sens. Environ., 113(12), 2642–2650, doi:10.1016/j.rse.2009.07.022, 2009.

Mishchenko, M. I. and Travis, L. D.: Satellite retrieval of aerosol properties over the ocean using polarization as well as intensity of reflected sunlight, J. Geophys. Res., 102(D12), 16989, doi:10.1029/96JD02425, 1997.

Remer, L. A., Knobelspiesse, K., Zhai, P., Xu, F., Kalashnikova, O. V., Chowdhary, J., Hasekamp, O., Dubovik, O., Wu, L., Ahmad, Z., Boss, E., Cairns, B., Coddington, O., Davis, A. B., Dierssen, H. M., Diner, D. J., Franz, B., Frouin, R., Gao, B., Ibrahim, A., Levy, R. C., Martins, J. V., Omar, A. H. and Torres, O.: Retrieving Aerosol Characteristics From the PACE Mission, Part 2: Multi-Angle and Polarimetry, Front. Environ. Sci., 7(July), 1–21, doi:10.3389/fenvs.2019.00094, 2019.

Stamnes, S., Hostetler, C., Ferrare, R., Burton, S., Liu, X., Hair, J., Hu, Y., Wasilewski, A., Martin, W., van Diedenhoven, B., Chowdhary, J., Cetinić, I., Berg, L. K., Stamnes, K. and Cairns, B.: Simultaneous polarimeter retrievals of microphysical aerosol and ocean color parameters from the "MAPP" algorithm with comparison to high-spectral-resolution lidar aerosol and ocean products, Appl. Opt., 57(10), 2394, doi:10.1364/AO.57.002394, 2018.

Wanner, W., Li, X. and Strahler, a H.: Kernel-driven models for the bidirectional reflectance dis- contain only geometric terms but no physical parameters . function land surfaces attempt The complete model then is linear be scaled to ar- to describe the BRDF as a linear superposition of a set, J. Geophys. Res., 100(D10), 21077–21089 [online] Available from: http://www.agu.org/pubs/crossref/1995/95JD02371.shtml, 1995.

Waquet, F., Léon, J. F., Cairns, B., Goloub, P., Deuzé, J. L. and Auriol, F.: Analysis of the spectral and angular response of the vegetated surface polarization for the purpose of aerosol remote sensing over land, Appl. Opt., 48(6), 1228–1236, doi:10.1364/AO.48.001228, 2009.

Xu, F., van Harten, G., Diner, D. J., Kalashnikova, O. V., Seidel, F. C., Bruegge, C. J. and Dubovik, O.: Coupled retrieval of aerosol properties and land surface reflection using the Airborne Multiangle SpectroPolarimetric Imager, J. Geophys. Res. Atmos., 122(13), 7004–

7026, doi:10.1002/2017JD026776, 2017.

Xu, F., Diner, D. J., Dubovik, O. and Schechner, Y.: A correlated multi-pixel inversion approach for aerosol remote sensing, Remote Sens., 11(7), doi:10.3390/rs11070746, 2019.